Control of the polarization of isolated attosecond pulses in atoms with nonvanishing angular quantum number

Candong Liu* and Mauro Nisoli

Department of Physics, Politecnico di Milano, National Research Council of Italy, Institute of Photonics and Nanotechnologies (CNR-IFN), Piazza L. da Vinci 32, I-20133 Milano, Italy

(Received 17 November 2011; published 27 January 2012)

High-order harmonic generation in the model hydrogenlike system He^+ prepared in an initial $2p_0$ state with nonvanishing angular quantum number is investigated by numerically solving the fully three-dimensional time-dependent Schrödinger equation. It is found that isolated attosecond pulses with elliptical polarization can be generated by using linearly polarized driving fields. The ellipticity, the major axis direction, and the helicity of the elliptically polarized attosecond pulses can be easily controlled by changing the polarization direction and the peak intensity of the driving pulses. It is shown that the resulting polarization state is related to the tunnel ionization step in the harmonic-generation process. Moreover, by using a simple analytical model it is demonstrated that the atomic nonvanishing angular momentum of the atomic medium used for harmonic generation plays a crucial role.

DOI: 10.1103/PhysRevA.85.013418 PACS number(s): 32.80.Rm, 42.65.Ky, 42.65.Re

I. INTRODUCTION

The central topic of attosecond science is the direct observation and control of ultrafast electron dynamics in atoms, molecules, and solids [1,2]. High-order harmonic generation (HHG) in atoms and molecules driven by an intense laser field supplies an effective way to produce attosecond pulses [3]. The underlying dynamics of HHG can be described by a simple semiclassical three-step model [4], which includes tunnel ionization, acceleration of the freed electron in the driving laser field, and recombination, with emission of subfemtosecond bursts of XUV photons. This process takes place every half-optical-cycle of the driving radiation, thus leading to the generation of trains of attosecond pulses [5]. Various gating schemes have been employed to confine the harmonic generation process to a single event, thus producing isolated attosecond pulses [6]: (i) spectral selection of the high-photon energy region of the XUV spectrum generated by sub-5-fs pulses [7]; (ii) use of driving pulses characterized by linear polarization in a short temporal window, where harmonic generation is allowed (polarization gating with one- [8,9] or two-color [10] excitation); and (iii) use of few-cycle pulses with above-saturation intensity [11]. The control of the temporal characteristics of the isolated attosecond pulses, in terms of pulse duration, central photon energy, and spectral chirp, is an important requisite for the applications of such pulses. Isolated attosecond pulses have been generated in various spectral regions upon using different gases for HHG and suitable spectral filtering elements. Ultrabroadband dispersion compensation has been demonstrated by using metallic filters [9,12] and propagation in plasma [13]. Another important characteristic is the polarization state: so far only linearly polarized isolated attosecond pulses have been generated. The control of the polarization characteristics of isolated attosecond pulses (i.e., ellipticity, major axis direction, and helicity) might open avenues for applications in probing ultrafast electron dynamics. However, there are no steadily available optical elements for polarization control in the extreme ultraviolet region.

Various techniques have been proposed and partly implemented for the generation of extreme ultraviolet (XUV) pulses with elliptical polarization. All methods rely on the common general idea that elliptically polarized harmonics can be produced by breaking the axial symmetry of the system. Borca *et al.* showed that by combining a static electric field and a linearly polarized driving pulse it is possible to achieve a significant control over the polarization properties of harmonics [14]. Elliptically polarized harmonics have been generated in aligned N_2 molecules, excited by linearly polarized laser fields [15]. Two-color field schemes have been proposed for the production of circularly polarized harmonics [16]. Ruiz *et al.* suggested the use of a two-color (ω, 1.5ω) scheme, where the two field components are linearly polarized and orthogonal to each other [17]. As for the single attosecond pulse generation, traditional studies in both experiments and theories are mainly focused on the pulse intensity and duration. Besides, the target gas atom is always the ground state or the excited s state with vanishing angular quantum number.

In this work, we investigate the polarization characteristics of isolated attosecond pulses generated in hydrogenlike systems characterized by atomic orbitals $\psi_{n\ell m}$ with $\ell \neq 0$. In particular we will concentrate on the atomic ion He^+ prepared in the $2p_0$ state, and excited by few-optical-cycle driving pulses with linear polarization to produce XUV radiation by HHG. By using numerical simulations we show that isolated attosecond pulses with elliptical polarization can be generated. Moreover we demonstrate that such polarization state is related to the tunnel ionization step in the harmonic-generation process from atomic orbitals with nonvanishing angular quantum momentum. Upon changing the polarization direction of the driving pulse the ellipticity, the major axis direction, and the helicity of the elliptically polarized attosecond pulses correspondingly change. We point out that He^+ in the $2p_0$ state can be prepared by exciting helium with linearly polarized π pulses, which can be designed to obtain a complete population transfer from the $1s$ to the $2p$ atomic orbital.

*cdliu@siom.ac.cn

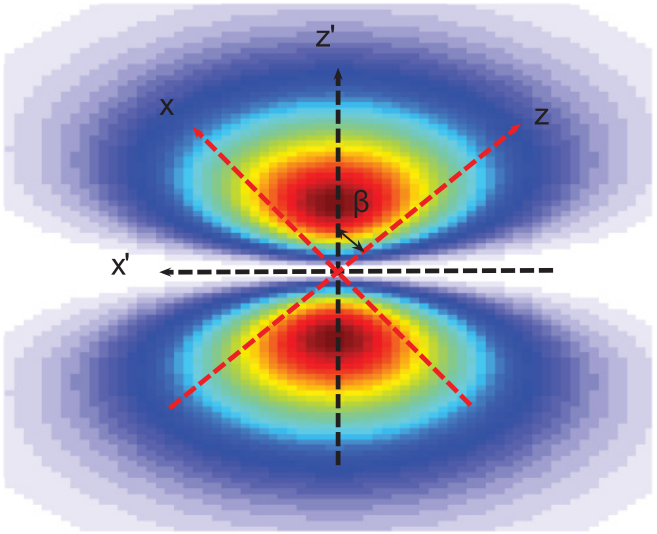

FIG. 1. (Color online) Electron probability density distribution of He^+ $2p_0$ state in the fixed (x',y',z') coordinate system. The polarization direction of the driving field is represented by the z axis, which forms the angle β with z' axis.

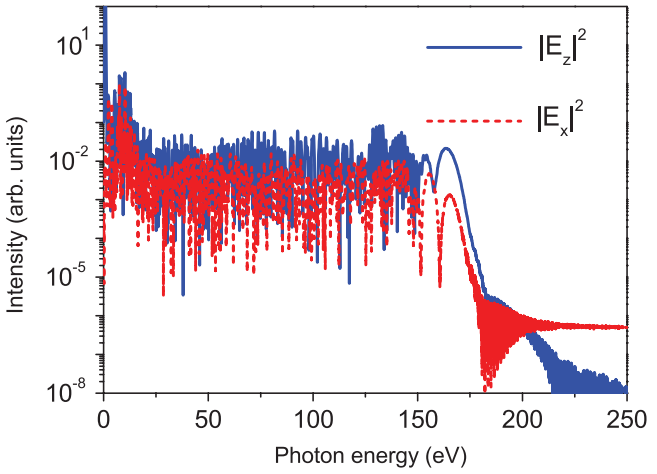

FIG. 2. (Color online) Harmonic spectra corresponding to the XUV field components along the x and z axes, calculated in He^+ in the $2p_0$ initial state by linearly polarized ($\beta = 45°$) 10-fs pulses, with central wavelength of 1.6 μm and peak intensity $I = 2 \times 10^{14}$ W/cm^2.

II. RESULTS AND DISCUSSION

Figure 1 shows the distribution of the electron probability density of the $2p_0$ state of He^+ in a fixed coordinate system (x',y',z'). The He^+ prepared atomic state $|\psi_{n_0,\ell_0,m_0}\rangle$ is the simultaneous eigenstate of L^2 and $L_{z'}$, where n_0, ℓ_0, m_0 are the main quantum number, the angular quantum number, and the magnetic quantum number respectively and L is the orbit angular-momentum operator. Note that the excited state $2p_0$ is characterized by a lifetime of the order of 100 ps [18]. The electron probability density of $|\psi_{n_0,\ell_0,m_0}\rangle$, with $n_0 = 2$, $\ell_0 = 1$, and $m_0 = 0$, is rotationally symmetric with respect to the z' axis. Therefore we can assume that the polarization direction of the driving field, represented by the z axis in Fig. 1 forming an angle β with z', lies in the $x'-z'$ plane without loss of generality. In order to conveniently solve the three-dimensional time-dependemt Schrödinger equation (3D-TDSE) by using the discrete variable representation (DVR) method [19,20], the initial state $|\psi_{n_0,\ell_0,m_0}\rangle$ is projected onto the xyz coordinate space because the angular-momentum component along the z axis is conserved. Therefore the initial wave function can be written as

$$\psi_{n_0,\ell_0,m_0}(r,\theta,\varphi) = R_{n_0,\ell_0}(r) \sum_{m'} d^{(\ell_0)}_{m',m_0}(\beta)\, Y^{m'}_{\ell_0}(\theta,\varphi), \quad (1)$$

where $R_{n_0,\ell_0}(r)$, $d^{(\ell_0)}_{m',m_0}(\beta)$, and $Y^{m'}_{\ell_0}(\theta,\varphi)$ are the normalized hydrogenic bound state radial wave function, the rotation matrix element, and the spherical harmonics, respectively. Here (r,θ,φ) are the spherical coordinates in xyz space. The temporal evolution of the wave function is obtained by the Arnoldi scheme [21]. The high-harmonic field is proportional to the Fourier transform of the dipole acceleration expectation value. We assumed a linearly polarized driving pulse with Gaussian intensity envelope, duration 10 fs and central wavelength 1600 nm. We have chosen a fundamental wavelength in the infrared region in order to increase the cutoff photon energy of the generated harmonic radiation, to reduce the attochirp [22], and to enhance phase matching [23], which is useful for the generation of isolated attosecond pulses. The laser parameters used in the simulations are experimentally realistic (see, for example, Ref. [24]).

A. HHG in $2p_0$ state

We have first calculated the XUV spectra produced in He^+ ions in the $2p_0$ state by linearly polarized pulses, with polarization direction forming an angle $\beta = 45°$ with the z' axis and peak intensity $I = 2 \times 10^{14}$ W/cm^2. The calculated intensity spectra corresponding to the XUV field components along the z and x axes are shown in Fig. 2; the harmonic signal along the y axis is zero. An important feature of the harmonic field is the nonvanishing x component, perpendicular to the polarization direction of the driving field. The intensity spectra shown in Fig. 2 are characterized by the same cut-off position. By selecting the cut-off harmonic spectrum above 165 eV and performing an inverse Fourier transform, it is possible to produce isolated attosecond pulses, with a duration of $\sim$360 as. The temporal evolution of the corresponding electric field is shown in Fig. 3(a): the pulse is elliptically polarized over its entire duration. The ellipticity e, defined as the ratio between the minor and major polarization ellipse axis, is $e \sim 0.12$. Figure 3(b) shows the electric field of the generated attosecond pulses, projected onto the E_z-E_x plane, characterized by a positive helicity (clockwise rotation of the electric field vector); the angle α between the major axis of the polarization ellipse and the positive E_z axis is $\alpha \approx 15°$.

We have then varied the polarization axis of the driving pulse, by changing β between 0 and 180°. Elliptically polarized isolated attosecond pulses can be produced by selecting the cut-off region of the harmonic spectrum, for all values of β. However, both the ellipticity e and the major axis direction are correspondingly changed. Figure 4(a) shows the ellipticity of

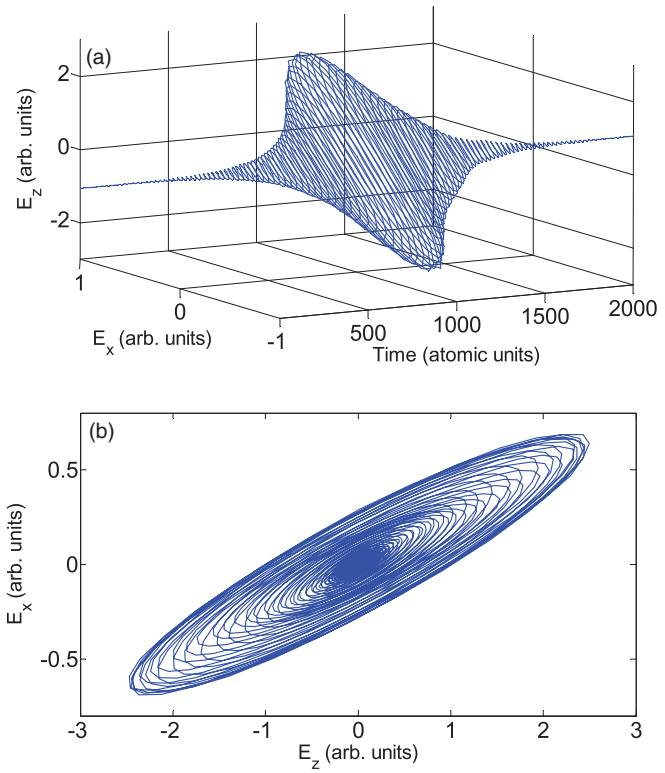

FIG. 3. (Color online) Isolated attosecond pulses produced by selecting the XUV components above 165 eV of the spectra reported in Fig. 2: (a) temporal evolution of the electric field; (b) projection of the electric field onto the E_z-E_x plane.

the isolated attosecond pulses as a function of β, calculated for two peak intensities of the the driving pulse: $I = 1.5 \times 10^{14}$ W/cm^2 (squares) and $I = 2 \times 10^{14}$ W/cm^2 (dots). Linearly polarized attosecond pulses can only be obtained when the electron density distribution is symmetric with respect to the polarization axis of the driving radiation ($\beta = 0$ and $\beta = 90^\circ$).

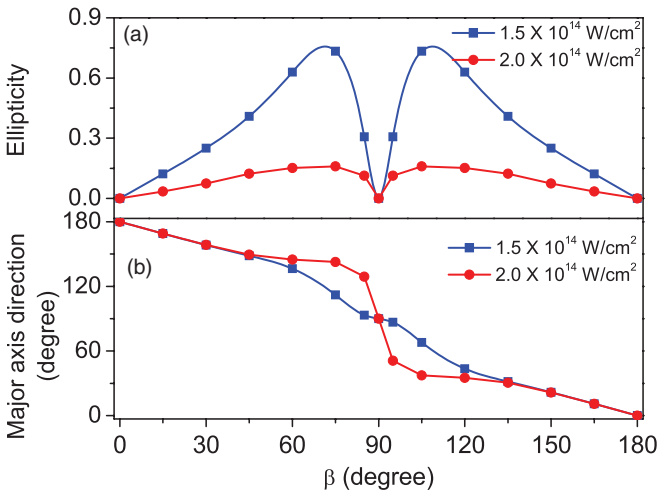

FIG. 4. (Color online) Ellipticity (a) and major axis direction (b) of the isolated attosecond pulses as a function of the polarization direction, β, of the driving field, calculated in the case of two excitation peak intensities: $I = 1.5 \times 10^{14}$ W/cm^2 (blue squares) and $I = 2 \times 10^{14}$ W/cm^2 (red dots).

Due to the symmetry of the initial electron density distribution, the ellipticity turns out to be symmetric with respect to $\beta = 90^\circ$. For a given value of β, the ellipticity increases upon decreasing the driving peak intensity, so that the use of driving pulses with moderate intensity allows one to tune in a broad region the ellipticity of the isolated attosecond pulses. Figure 4(b) displays the corresponding variation of major axis direction, defined as the angle of counterclockwise rotation from the positive z' axis to the major axis of the polarization ellipse. One can see that the major axis direction is almost insensitive to the laser intensity variation for $\beta < 60^\circ$ (and $\beta > 120^\circ$). Moreover, the helicity of the electric field of the elliptically polarized attosecond pulse is positive (clockwise rotation) for $\beta < 90^\circ$ and negative (counterclockwise rotation) for $\beta > 90^\circ$ on the $x'z'$ plane.

B. Strong-field approximation model

In order to understand the physical processes at the basis of the generation of attosecond pulses with tunable elliptical polarization from electronic states with nonvanishing angular quantum number, we have used the strong-field approximation (SFA), which offers a neat physical picture for the investigation of the HHG process. The harmonic field $\mathbf{H}(\omega)$ at frequency ω is proportional to the transition dipole moment between the bound state and the continuum electron [25]

$$\mathbf{H}(\omega) \propto \langle \psi_{n_0\ell_0 m_0} | \mathbf{r} | \exp[i\mathbf{k}(\omega)\cdot\mathbf{r} + i\gamma(\omega, I_0)] \rangle, \tag{2}$$

where $\psi_{n_0\ell_0 m_0}$ is the initial bound state, $\exp[i\mathbf{k}(\omega)\cdot\mathbf{r} + i\gamma(\omega, I_0)]$ is the plane wave propagating along the driving field direction, I_0 is the driving peak intensity contributing to the cut-off region of harmonic spectrum, $\gamma(\omega, I_0)$ refers to the atomic phase accumulation in the external field, and $\mathbf{k}(\omega)$ is the wave number corresponding to the harmonic frequency ω. The harmonic components along x, y, and z axes (see Fig. 1) can be expressed as

$$H_z(\omega) \propto f_{m'=0}(\beta, I_0), \tag{3a}$$

$$H_x(\omega) \propto \sum_{m'=-\ell_0}^{\ell_0} (\delta_{m',1} + \delta_{m',-1}) g_{m'}(\beta, I_0), \tag{3b}$$

$$H_y(\omega) \propto i \sum_{m'=-\ell_0}^{\ell_0} (\delta_{m',1} - \delta_{m',-1}) g_{m'}(\beta, I_0), \tag{3c}$$

where

$$f_{m'}(\beta, I_0) = \int dr d\theta\, r^2 \sin\theta\, R_{n_0,\ell_0}\, d^{(\ell_0)}_{m' m_0}(\beta)\, P^{m'}_{\ell_0}\, r\cos\theta \times \exp[-ikr\cos\theta - i\gamma(\omega, I_0)], \tag{4}$$

and

$$g_{m'}(\beta, I_0) = \int dr d\theta\, r^2 \sin\theta\, R_{n_0,\ell_0}\, d^{(\ell_0)}_{m' m_0}(\beta)\, P^{m'}_{\ell_0}\, r\sin\theta \times \exp[-ikr\cos\theta - i\gamma(\omega, I_0)], \tag{5}$$

are complex numbers with an amplitude and a phase. One can easily see that when the initial angular quantum number is $\ell_0 = 0$, so that the s state is used to produce high-order harmonics in a driving field with linear polarization, the harmonic emission perpendicular to the polarization axis of the driving

field disappears ($H_x = H_y = 0$). Consequently, the attosecond pulses that are produced by synthesizing harmonic spectrum are usually linearly polarized. Elliptically polarized attosecond pulses can be generated when atomic states with nonvanishing angular quantum number ($\ell_0 > 0$) are used. Additionally, since the integration of H_i ($i = x,y,z$) over the selected high-harmonic spectrum are complex functions of both β and I_0, the ellipticity and the major axis direction can be controlled by varying the polarized direction β and the peak intensity I_0 of the driving pulse. We point out that this simple analytical model demonstrates that the polarization control is not dependent on the specific atomic species, but relates to the angular quantum number ($\ell_0 > 0$), so that any atomic system with nonvanishing internal angular momentum can be used to generate elliptically polarized isolated attosecond pulses, with controllable ellipticity.

C. Tunnel ionization

The generation of an XUV field component (H_x) in a direction perpendicular to the polarization axis of the driving field can be qualitatively understood by analyzing the motion of the electronic wave packet after tunnel ionization from the initial $2p_0$ state. We point out that in the case of tunnel ionization from spherically symmetric ground state, the corresponding electron wave packet always spreads along the electric field direction, in the case of linearly polarized driving pulses, thus leading to the generation of linearly polarized high-order harmonic radiation. The expectation value of the electron motion perpendicular to the driving electric field can be defined as $\bar{x}(t) = \langle\psi(r,\theta,\varphi,t)|x|\psi(r,\theta,\varphi,t)\rangle$, which represents the extent of electron ionization deviating from the driving electric field direction. The time-dependent wave function $\psi(r,\theta,\varphi,t)$ is directly obtained from the TDSE. Figure 5 shows the calculated average electron motion in the x direction induced by a driving field polarized along the z direction, with $\beta = 45^\circ$ and peak intensity $I_0 = 2 \times 10^{14}$ W/cm^2. The origin of this lateral shift can be attributed to the internal angular momentum $\sqrt{\ell_0(\ell_0+1)}\hbar$ in the $2p_0$ state. The dipole acceleration in the x direction leads to the generation of elliptically polarized XUV pulses. We have then performed a series of calculations by varying the laser intensity and the polarization angle β of the driving field: the electron motion in the x direction turns out to depend on both parameters. In perfect agreement with the results of the 3D-TDSE shown in Fig. 4, the transverse electron drift increases upon decreasing the driving intensity. This result can be interpreted as follows: The force experienced by the freed electron increases upon increasing the driving peak intensity, so that at high intensities

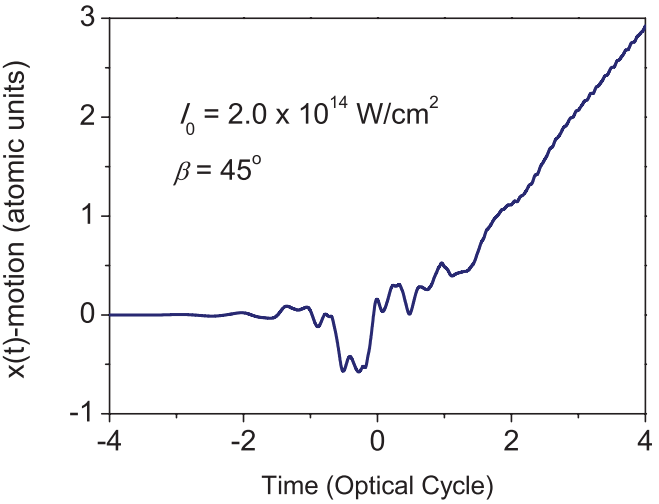

FIG. 5. (Color online) Expectation value of electron x direction lateral motion as a function of time. The driving pulse has a polarized direction $\beta = 45^\circ$ and a peak intensity of $I = 2 \times 10^{14}$ W/cm^2.

the electron motion after tunnel ionization is predominantly in the polarization direction of the driving field. In this case the emitted harmonic radiation is characterized by low ellipticity, in agreement with Fig. 4(a).

III. CONCLUSIONS

In conclusion, we demonstrated that the model hydrogenlike system He^+, prepared in an initial $2p_0$ state with nonvanishing angular momentum, driven by few-optical-cycle pulses can be used for the generation of isolated attosecond pulses with elliptical polarization. We found that the ellipticity and the major axis direction of the polarization ellipse can be continuously tuned upon changing the peak intensity and the polarization direction of the driving field. This offers a simple method to control the attosecond pulse polarization, which is generally difficult to achieve by using traditional schemes. A simple analytical model based on SFA shows that the atomic nonvanishing angular momentum is the prerequisite for this kind of polarization control.

ACKNOWLEDGMENTS

This research was supported by the European Research Council under the European Community's Seventh Framework Programme (FP7/2007-2013)/ERC Grant Agreement No. 227355 ELYCHE, the European Union under Contract No. 228334 JRA-ALADIN (Laserlab Europe II), and the MC-RTN ATTOFEL (FP7-238362).

[1] F. Krausz and M. Ivanov, Rev. Mod. Phys. **81**, 163 (2009).
[2] M. Nisoli and G. Sansone, Prog. Quantum Electron. **33**, 17 (2009).
[3] P. B. Corkum and F. Krausz, Nature Phys. **3**, 381 (2007).
[4] P. B. Corkum, Phys. Rev. Lett. **71**, 1994 (1993).
[5] P. M. Paul, E. S. Toma, P. Breger, G. Mullot, F. Augé, Ph. Balcou, H. G. Muller, and P. Agostini, Science **292**, 1689 (2001).
[6] F. Calegari, F. Ferrari, M. Lucchini, M. Negro, C. Vozzi, S. Stagira, G. Sansone, and M. Nisoli, in *Advances in Atomic, Molecular, and Optical Physics*, edited by E. Arimondo, P. R. Berman, and C. C. Lin, Vol. 60 (Academic Press, San Diego, 2011), pp. 371–413.
[7] M. Hentschel, R. Kienberger, Ch. Spielmann, G. A. Reider, N. Milosevic, T. Brabec, P. Corkum, U. Heinzmann,

M. Drescher, and F. Krausz, Nature (London) **414**, 509 (2001).
[8] I. J. Sola, E. Mével, L. Elouga, E. Constant, V. Strelkov, L. Poletto, P. Villoresi, E. Benedetti, J.-P. Caumes, S. Stagira, C. Vozzi, G. Sansone, and M. Nisoli, Nature Phys. **2**, 319 (2006).
[9] G. Sansone, E. Benedetti, F. Calegari, C. Vozzi, L. Avaldi, R. Flammini, L. Poletto, P. Villoresi, C. Altucci, R. Velotta, S. Stagira, S. De Silvestri, and M. Nisoli, Science **314**, 443 (2006).
[10] H. Mashiko, S. Gilbertson, C. Li, S. D. Khan, M. M. Shakya, E. Moon, and Z. Chang, Phys. Rev. Lett. **100**, 103906 (2008).
[11] F. Ferrari, F. Calegari, M. Lucchini, C. Vozzi, S. Stagira, G. Sansone, and M. Nisoli, Nature Phot. **4**, 875 (2010).
[12] Rodrigo López-Martens, K. Varjú, P. Johnsson, J. Mauritsson, Y. Mairesse, P. Salières, M. B. Gaarde, K. J. Schafer, A. Persson, S. Svanberg, C.-G. Wahlström, and A. L'Huillier, Phys. Rev. Lett. **94**, 033001 (2005).
[13] K. T. Kim, K. S. Kang, M. N. Park, T. Imran, G. Umesh, and C. H. Nam, Phys. Rev. Lett. **99**, 223904 (2007).
[14] B. Borca, A. V. Flegel, M. V. Frolov, N. L. Manakov, D. B. Milošević, and A. F. Starace, Phys. Rev. Lett. **85**, 732 (2000).
[15] X. Zhou, R. Lock, N. Wagner, W. Li, H. C. Kapteyn, and M. M. Murnane, Phys. Rev. Lett. **102**, 073902 (2009).
[16] D. B. Milošević, W. Becker, and R. Kopold, Phys. Rev. A **61**, 063403 (2000).
[17] C. Ruiz, D. J. Hoffmann, R. Torres, L. E. Chipperfield, and J. P. Marangos, New J. Phys. **11**, 113045 (2009).
[18] G. W. F. Drake, J. Kwela, and A. van Wijngaarden, Phys. Rev. A **46**, 113 (1992).
[19] L. Peng and A. F. Starace, J. Chem. Phys. **125**, 154311 (2006).
[20] K. Dunseath, J. Launay, M. Dunseath, and L. Mouret, J. Phys. B **35**, 3539 (2002).
[21] T. J. Park and J. C. Light, J. Chem. Phys. **85**, 5870 (1986).
[22] J. Tate, T. Auguste, H. G. Muller, P. Saliéres, P. Agostini, and L. F. DiMauro, Phys. Rev. Lett. **98**, 013901 (2007).
[23] V. S. Yakovlev, M. Ivanov, and F. Krausz, Opt. Express **15**, 15351 (2007).
[24] B. Schmidt, P. Béjot, M. Giguére, A. D. Shiner, C. Herrero, E. Bisson, J. Kasparian, J. Wolf, D. M. Villeneuve, J. Kieffer, P. B. Corkum, and F. Légaré, Appl. Phys. Lett. **96**, 121109 (2010)
[25] J. Itatani, J. Levesque, D. Zeidler, H. Niikura, H. Pépin, J. C. Kieffer, P. B. Corkum, and D. M. Villeneuve, Nature (London) **423**, 867 (2004).